Correlation between Multiple Hydrogen Bonding and Alteration of the Oxidation Potential of the Bacteriochlorophyll Dimer of Reaction Centers from *Rhodobacter sphaeroides*†

T. A. Mattioli,*,‡ X. Lin,§ J. P. Allen,§ and J. C. Williams§

Section de Biophysique des Protéines et des Membranes, Département de Biologie Cellulaire et Moléculaire, CEA and URA CNRS 1290, C.E. de Saclay, 91191 Gif-sur-Yvette Cedex, France, and Department of Chemistry and Biochemistry and the Center for the Study of Early Events in Photosynthesis, Box 871604, Arizona State University, Tempe, Arizona 85287-1604

Received December 20, 1994; Revised Manuscript Received March 7, 1995⊗

ABSTRACT: The electronic absorption and vibrational Raman spectra of mutant reaction centers from *Rhodobacter sphaeroides* bearing multiple site-specific mutations near the primary electron donor (P), a bacteriochlorophyll dimer, are reported. These mutations bear double and triple combinations of single-point mutations that alter the H-bonding interactions between histidine residues and the C_2- and C_9-conjugated carbonyl groups of the primary donor [Mattioli, T. A., Williams, J. C., Allen, J. P., & Robert, B. (1994) *Biochemistry 33*, 1636−1643] and change the donor redox midpoint potential from 410 to 765 mV compared to 505 mV for wild type [Lin, X., Murchison, H. A., Nagarajan, V., Parson, W. W., Williams, J. C., & Allen, J. P. (1994) *Proc. Natl. Acad. Sci. U.S.A. 91*, 10265−10269]. Near-infrared Fourier transform Raman spectroscopy was used to determine the changes in H-bonding interactions of the primary donor in these multiple mutants. The Fourier transform Raman spectra of the mutants exhibit the predicted changes in hydrogen bond interactions of the P carbonyl groups with the protein, and they are consistent with the designed mutations. Moreover, the Raman data verify that the H-bonds formed or broken in the multiple mutants are similar in strength to those observed in the corresponding single mutants. A correlation was observed between the change in $P/P^{\bullet+}$ redox midpoint potential and the total change in H-bonding interaction energy (from −207 to 364 meV relative to wild type) as gauged by the estimated enthalpy of each H-bond formed or broken on the four conjugated carbonyls of the primary donor. Only minor changes were observed in the optical spectra of the mutant reaction centers, indicating that the addition of H-bonds from histidines has little effect in destabilizing the first electronic excited state of the dimer relative to the ground state. However a blue shift in the dimer absorption band at *ca.* 890 nm at 20 K was associated with the removal of the H-bond to the C_2 acetyl carbonyl group via His L168. A red shift of the oxidized dimer band at *ca.* 1250 nm was associated with the formation of each H-bond to the C_9 keto carbonyl groups.

The reaction center (RC[1]) of photosynthetic systems is the membrane-spanning protein which contains the pigments that are responsible for the primary light reactions. Several types of RCs are known [see review in Nitschke and Rutherford (1991)], but the role of the chlorophyllic cofactors they harbor remains the same: light-driven redox chemistry resulting in stable, transmembrane charge separation. In order to optimize this primary process, the pigments in the RC must exhibit compatible light absorption properties and compatible redox potentials to match the thermodynamics of the subsequent electron transfer chain.

One crucial redox component in the RC is the primary electron donor, P. Electron transfer is initiated following the excitation of P, and thus its physicochemical properties are expected to play a significant role in the initial redox reactions (Lin *et al.*, 1994a). In particular, the oxidation potential of P is expected to be an important parameter in the electron transfer reactions involving P, as it will in part define the driving force of these reactions. These driving forces are presumably optimized in the protein in the initial electron transfer processes, and the redox potential of the primary donor should be compatible with the redox potentials of the subsequent electron-carrying cofactors. For example, the RCs of both photosystems I and II (PSI and PSII, respectively) contain chlorophyll *a* (Chl *a*) pigments but operate at different redox potential scales. The PSII RC must operate at relatively high potentials in order to oxidize water, and yet the RC of PSI must reduce ferredoxin. The redox potential of the primary donor of PSI is approximately 500 mV, while that of PSII is over 1 V. This difference in redox potential for the PSII and PSI primary donors is thought to be largely due to the extent of their monomeric and dimeric $(Chl\ a)_2$ nature, respectively; however, other protein factors must certainly be at play which elevate the redox potential of P680 to values greater than that observed for Chl *a in*

† This work was supported by grants from the National Institutes of Health (GM45902) and the National Science Foundation (MCB9404925). This is publication No. 231 from the Center for the Study of Early Events in Photosynthesis.

* Corresponding author. Fax: 33-1-6908 4389. e-mail: mattioli@tobit.saclay.cea.fr.

‡ CEA and URA CNRS 1290.

§ Arizona State University.

⊗ Abstract published in *Advance ACS Abstracts,* April 15, 1995.

[1] Abbreviations: FT, Fourier transform; RR, resonance Raman; P, primary electron donor; RC, reaction center; *Rb.*, *Rhodobacter*; WT, wild type; BChl, bacteriochlorophyll; BPhe, bacteriopheophytin; Tris, tris(hydroxymethyl)aminomethane; EDTA, ethylenediaminetetraacetic acid; LDAO, lauryldimethylamine *N*-oxide.

0006-2960/95/0434-6142$09.00/0

vitro (Watanabe & Kobayashi, 1991). Similarly, the primary donor of the green sulfur bacteria (*i.e.*, *Chlorobium*) consists of a dimer of bacteriochlorophyll *a* molecules [see review by Feiler and Hauska (1994)], as in *Rhodobacter sphaeroides* and other purple bacteria, yet the redox midpoint potential is more than 200 mV lower than that of purple bacteria. The specific interactions of the pigments and the protein which modulate these physicochemical properties of the primary electron donors are still not fully understood.

The RC from the purple photosynthetic bacterium *Rb. sphaeroides* noncovalently binds the pigment cofactors within two polypeptide subunits named L and M (Yeates *et al.*, 1988; El-Kabbani *et al.*, 1991; Chirino *et al.*, 1994; Ermler et al., 1994). The primary electron donor (P) in the *Rb. sphaeroides* RC is a dimer of bacteriochlorophyll *a* (BChl *a*) molecules (designated P_L and P_M) that overlap at ring I and are approximately 3.5 Å apart. With respect to the conjugated C_2 acetyl and C_9 keto carbonyl groups of P, only the acetyl carbonyl of P_L is engaged in a H-bond with the protein, the donor being His L168 (Allen *et al.*, 1987; El-Kabbani *et al.*, 1991; Chirino *et al.*, 1994; Ermler *et al.*, 1994; Mattioli *et al.*, 1991, 1994). The redox midpoint potential of the $P/P^{\bullet+}$ couple for isolated RCs is *ca.* 500 mV (Moss *et al.*, 1991; Williams *et al.*, 1992b; Nagarajan *et al.*, 1993; Jia *et al.*, 1994; Beekman *et al.*, 1995).

Recently, a series of RC mutants have been constructed to modify the H-bonding pattern on the conjugated carbonyl groups of P in *Rb. sphaeroides* by introducing histidine-donated H-bonds or removing that present in wild type (Williams *et al.*, 1992a; Murchison *et al.*, 1993; Lin *et al.*, 1994a). In the single-point mutations in *Rb. sphaeroides*, Leu to His at L131, LH(L131), Leu to His at M160, LH(M160), Phe to His at M197, FH(M197), and His to Phe at L168, HF(L168), the formation and removal of the H-bonds were confirmed using FT Raman (Mattioli *et al.*, 1994) as well as FTIR difference (Nabedryk *et al.*, 1993) vibrational spectroscopies.

In this paper, we present near-infrared FT Raman and optical absorption spectroscopic data of double and triple mutants of RCs from *Rb. sphaeroides* which alter the H-bonding pattern of the conjugated carbonyls of P. These multiple mutations correspond to combinations of the genetically introduced changes in H-bond interactions of the single mutants at positions L168, M197, M160, and L131. The FT Raman data presented here fully confirm the formation of these H-bonds and provide their strengths. It is found that the respective H-bonds in the double and triple mutants reported here have similar strengths as compared to those found for the single mutations. Thus, the total H-bonding interaction as gauged by the estimated H-bond enthalpies of each H-bond formed or broken on the four conjugated carbonyl groups of P correlates with the additive behavior of the changes in $P/P^{\bullet+}$ redox potentials (Lin *et al.*, 1994a,b). Furthermore, to a first approximation, this correlation is observed to be linear.

EXPERIMENTAL PROCEDURES

Mutagenesis, Bacterial Growth, and RC Isolation. The constructions of the single mutants LH(L131), LH(M160), HF(L168), and FH(M197) and the double mutant LH(L131) + LH(M160) have been reported elsewhere (Williams *et al.*, 1992a,b; Murchison *et al.*, 1993; Lin *et al.*, 1994a). Construction of the double and triple mutants LH(M160) + FH(M197), LH(L131) + HF(L168), HF(L168) + LH(M160), HF(L168) + FH(M197), and LH(L131) + LH(M160) + FH(M197) is described in Lin *et al.* (1994a). The triple mutant HF(L168) + LH(L131) + LH(M160) was constructed in a manner similar to that described for the other double and triple mutants, by combining a restriction fragment containing the two mutations in the L subunit gene with a fragment containing the mutation in the M subunit gene. The mutants were grown under nonphotosynthetic conditions, and RCs were isolated using procedures described previously (Williams *et al.*, 1992b).

Isolated RCs were prepared in 15 mM Tris-HCl buffer, pH 8, 1 mM EDTA, and 0.025% LDAO. RC samples were concentrated to *ca.* 100 OD at 860 nm using a Centricon microconcentrator system (Amicon).

Fourier Transform Raman Spectroscopy. The FT Raman spectra of RCs, at room temperature, were recorded using a Bruker IFS 66 interferometer coupled to a Bruker FRA 106 Raman module as described elsewhere (Mattioli *et al.*, 1991, 1994). The RCs were poised in their P° or $P^{\bullet+}$ states by addition of ascorbate or ferricyanide, respectively. Mutant RCs which could not be completely oxidized with ferricyanide treatment were illuminated with white light (*ca.* 150 W) for *ca.* 1 min, rapidly frozen at 77 K, and then transfered to a cold helium gas-circulating cryostat (Mattioli *et al.*, 1994). Spectra of these samples were recorded at 15 K and compared, under the same experimental and geometric conditions, to those not illuminated. For the FH(M197) + LH(L131) + LH(M160) triple mutant, we were unable to generate a sizeable amount of the $P^{\bullet+}$ state either by ferricyanide addition at room temperature or by low-temperature trapping after illumination due to its greatly decreased yield of charge separation (Woodbury *et al.*, 1995).

Optical Spectroscopy. Optical absorption spectra of isolated, reduced RCs were recorded using a Cary 5 spectrophotometer (Varian) at room and low (20 K) temperatures. For low-temperature measurements, RCs were in 15 mM Tris-HCl, pH 8, 1 mM EDTA, and 0.025% LDAO with glycerol added to a final concentration of 67% (v/v). Samples were cooled to cryogenic temperatures using a 1.5 mm path length sample holder with quartz windows mounted to the cold tip of a helium displex refrigerator and measured as described elsewhere (Williams *et al.*, 1992b).

Near-IR Absorption Spectroscopy. Room temperature absorption spectra in the 700−1300 nm region of isolated, oxidized RCs were recorded using the same Bruker IFS 66 interferometer as for the FT Raman experiments but in absorption mode (Wachtveitl *et al.*, 1993). Samples were held in a 1 cm quartz cell. The actinic effect of the measuring beam itself was used to photo-oxidize P; the fraction of RCs which were oxidized was varied by changing the position of the 1 cm cuvette containing the RC within the measuring beam. When the cuvette was positioned so that the measuring beam passed through the sample in an unfocused state, it was observed that *ca.* 15% of the RCs were in their $P^{\bullet+}$ state. Changing the sample position within the same measuring beam so that it passed through the sample in a focused state increased the actinic effect so that essentially 100% of the RCs were in their $P^{\bullet+}$ state. It was verified that these changes in sample position did not distort the resulting absorption spectra. During the recording of the

Table 1: Comparison of Observed Vibrational Frequencies for the C_2 and C_9 Carbonyl Groups of P, Change in Estimated H-Bond Enthalpies, and $P/P^{\bullet+}$ Midpoint Potentials for Dimer H-Bond Mutants

strain	C_2[b] (cm^{-1})		C_9[b] (cm^{-1})		$\Delta\Delta H$[c] (meV)	$P/P^{\bullet+}$ E_m (ΔE_m) (mV)[f]
	P_L	P_M	P_M	P_L		
WT[a]	1620	1653	1679	1691	0	505 (0)
HF(L168)[a]	1653	1653	1679	1688	−207	410 (−95)
FH(M197)[a]	1622	***1630***	1679	1693	145	630 (125)
LH(M160)[a]	1618	1657	***1657***	1694	138	565 (60)
LH(L131)[a]	1627	1657	1684	***1673***	70	585 (80)
LH(131) + LH(M160)[a]	1627	1657	***1657***	***1673***	208	635 (130)
HF(L168) + LH(L131)	1653	1653	1680	***1664***	−38	485 (−20)
HF(L168) + FH(M197)	1657	***1628***	1682	1689	−51	545 (40)
LH(M160) + FH(M197)	1618	***1639***	***1661***	1696	201	700 (195)
FH(M197) + LH(L131) + LH(M160)	1628	***1636***	***1663***	***1674***	364	765 (260)
HF(L168) + LH(L131) + LH(M160)[d]	1657	1657	***1657***	***1676***	25	540 (35)
HF(L168) + LH(L131) + LH(M160)[e]	1657	1657	***1668***	***1678***	−44	540 (35)

[a] Data from Mattioli *et al.* (1994). [b] Note: values which are underlined denote that they result from a H-bond rupture, while values in ***italicized boldface*** denote they result from H-bond formation. [c] Total change in the estimated H-bond enthalpies from each H-bond to the primary donor. The individual ΔH values for each single H-bond were determined using empirical Badger-type relation in Zadorozhnyi and Ishchenko (1965) relating ΔH with observed carbonyl frequency shift. Each individual ΔH value was added to give the total change in H-bond interaction energy. The ΔH estimated by the removal of the H-bond by His L168 to the acetyl carbonyl of P_L in wild type is taken as a negative value, by our convention. [d] Value of the 1676 cm^{-1} band as observed in the unresolved shoulder in the room temperature and low-temperature FT Raman spectra (see text for details). [e] Values of the 1668 and 1678 cm^{-1} bands as obtained from the spectral deconvolution of the *ca.* 1676 cm^{-1} shoulder in the room temperature FT Raman spectrum (see text for details). [f] Values from Lin *et al.* (1994a).

absorption spectrum of neutral P, ascorbate was added to ensure RCs were completely reduced.

RESULTS

FT Raman Spectra of the Reduced Primary Donor. We have previously shown that the room temperature FT preresonance Raman spectra of reduced RCs excited with 1064 nm radiation involve a preresonance enhancement of the vibrational spectrum of ground-state P via its *ca.* 865 nm lower excitonic Q_y absorption band (Mattioli *et al.*, 1991, 1993, 1994; Wachtveitl *et al.*, 1993). This preresonance condition is sufficiently pronounced so as to enhance the Raman contributions of P over those of the accessory BChl and BPhe molecules. The assignments of the C_2 acetyl and C_9 keto carbonyl stretching modes of P_L and P_M in the wild type strain of *Rb. sphaeroides* have been discussed elsewhere (Mattioli *et al.*, 1991, 1994) and are listed in Table 1. Table 1 also lists the frequencies of these carbonyl stretching modes for RCs with single mutations that resulted in either the removal of a H-bond on the acetyl carbonyl of P_L via His L168 or the formation of new H-bonds on the other C_2 and C_9 carbonyl groups via the genetic introduction of histidine residues (Mattioli *et al.*, 1994). The double and triple mutants reported in this work represent sets of combinations of these single mutations.

Figures 1 and 2 show the FT Raman spectra of reduced WT and double- and triple-mutant RCs from *Rb. sphaeroides*. The invariance of the *ca.* 1607 cm^{-1} band indicates that there is no change in the coordination number of the central Mg atom of the BChl *a* molecules constituting P. Table 1 indicates the observed vibrational frequencies of each of the C_2 and C_9 carbonyls of P as well as those for the single mutants. The FT Raman spectra of the double mutant LH(L131) + LH(M160) showed the formation of H-bonds to the C_9 keto carbonyls of both P_L and P_M, as described in Mattioli *et al.* (1994). These H-bonds resulted in downshifts of the P_L (−18 cm^{-1}) and P_M (−22 cm^{-1}) keto carbonyl stretching modes that are similar to those observed for the LH(L131) and LH(M160) single mutants, indicating that the H-bond strengths observed in the single mutations were conserved for the LH(L131) + LH(M160) double mutant. In general, the conservation of these and the other H-bond on the P_M C_2 acetyl carbonyl is observed in the double and triple mutants reported here (see below). The C_{10} carbomethoxy ester carbonyl groups are expected to contribute at *ca.* 1740 cm^{-1}. The wild type spectra shown in Figures 1 and 2 exhibit two weak bands at 1732 and 1741 cm^{-1} which could be assigned to these groups (Mattioli *et al.*, 1991; Wachtveitl *et al.*, 1993). These weak bands are not clearly observed in most of the mutant spectra reported here, due to the amount of inherent sample fluorescence which limits the signal-to-noise ratio of these spectra, and thus it is not possible to conclude if changes of H-bonding states with these C_{10} carbomethoxy ester carbonyl groups have occurred.

Double Mutants. The 1064 nm excited FT Raman spectrum of the primary donor in the HF(L168) + FH(M197) double mutant is shown in Figure 1. This mutant has been designed to place a H-bond on the C_2 acetyl carbonyl of P_M and remove that found in WT on the C_2 acetyl carbonyl of P_L, via His L168. On the basis of the assigned stretching frequencies of these carbonyl groups and previous work on the single mutants (Mattioli *et al.*, 1991, 1994), we expect the 1653 cm^{-1} band corresponding to the P_M acetyl carbonyl to downshift to *ca.* 1630 cm^{-1} and the 1620 cm^{-1} band of the P_L acetyl carbonyl to upshift to *ca.* 1653 cm^{-1}. The FT Raman spectrum of this mutant is consistent with these expectations, and we conclude that the changes in the designed H-bond interactions have occurred. There are also some minor perturbations, on the order of 3 cm^{-1} shifts, of the C_9 carbonyl stretching frequencies of P_L and P_M, which make them less resolved as compared to wild type. This spectrum appears very similar to that of WT since one H-bond on an acetyl carbonyl has been broken and another formed which exhibits an acetyl carbonyl frequency at 1628 cm^{-1}. We note however, as in the case of the single mutants HF(L168) and FH(M197), that the genetically introduced H-bond on the P_M acetyl carbonyl in the HF(L168) + FH(M197) double mutant is not as strong as that found on P_L

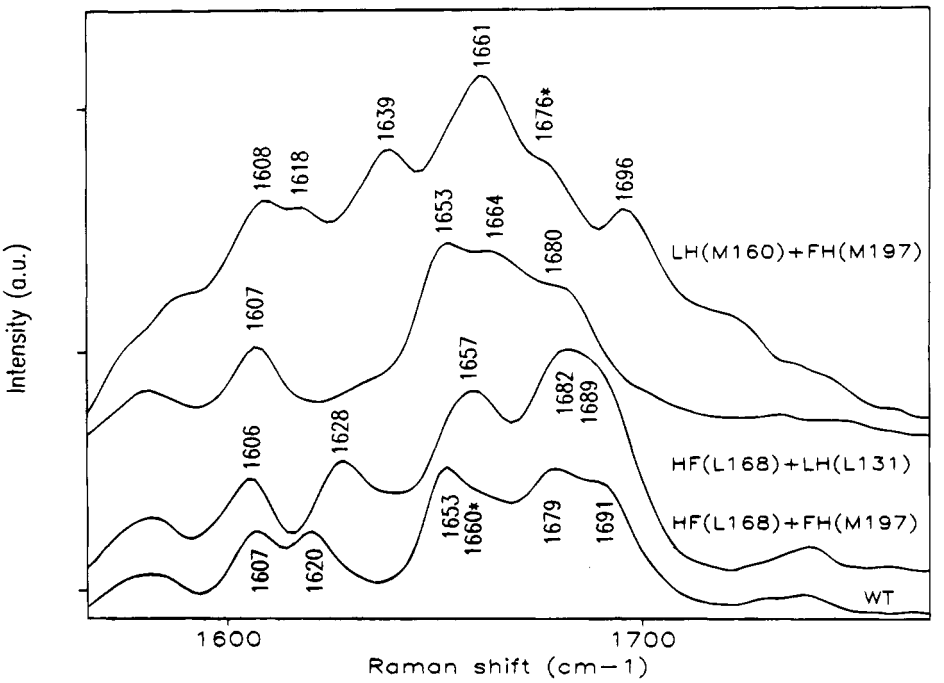

FIGURE 1: Room temperature P° FT preresonance Raman spectra of *Rb. sphaeroides* wild type and the double-hydrogen-bond mutant reaction centers. Reaction centers are poised in their P° state in the presence of ascorbate. The 1660(*) and 1676(*) cm^{-1} bands in the wild type and LH(M160) + FH(M197) spectra, respectively, do not arise from P. Excitation was at 1064 nm, with 180 mW of power, 4000 interferograms, and 4 cm^{-1} resolution.

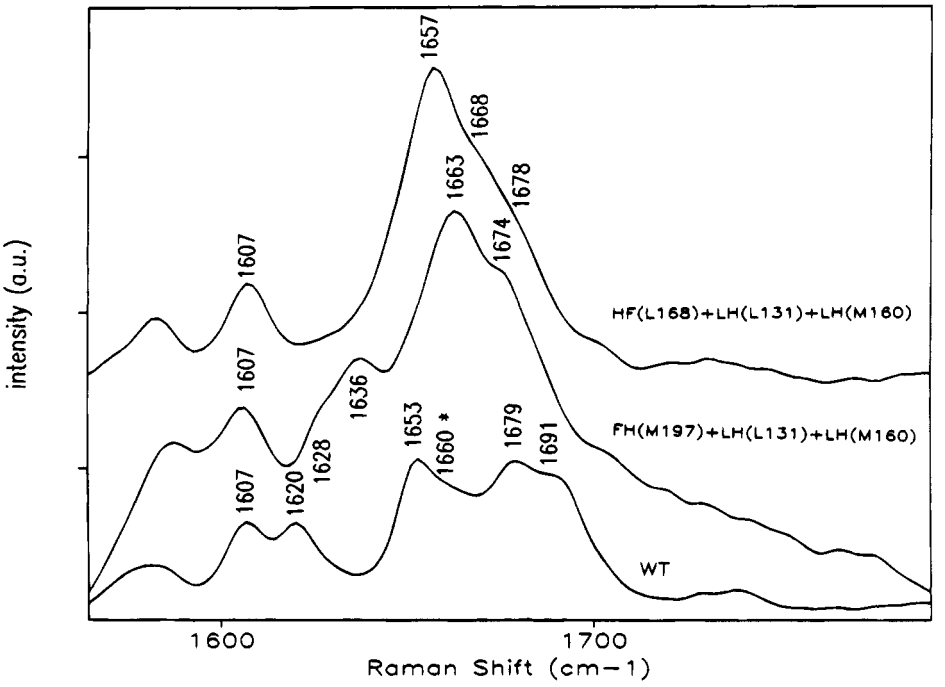

FIGURE 2: Room temperature P° FT preresonance Raman spectra of *Rb. sphaeroides* wild type and the triple-hydrogen-bond mutant reaction centers (same conditions as in Figure 1).

in WT and is easily distinguished by the 1628 cm^{-1} band (1620 cm^{-1} in WT spectrum).

The FT Raman spectrum of the HF(L168) + LH(L131) double mutant is also shown in Figure 1. This mutant was designed to place a H-bond on the C_9 keto carbonyl of P_L and remove that on the C_2 acetyl carbonyl of P_L. Again, on the basis of previous work with the single mutants, we expect the 1620 cm^{-1} band, corresponding to the C_2 acetyl carbonyl of P_L, to upshift to *ca.* 1653 cm^{-1} and the 1691 cm^{-1} band of the C_9 keto carbonyl of P_L to downshift to *ca.* 1673 cm^{-1}. The FT Raman spectrum of this mutant indeed confirms the formation and rupture of the above-mentioned H-bonds as is signalled by the absence of the 1620 and 1691 cm^{-1} bands and by a new band at 1664 cm^{-1}. The 1664 cm^{-1} band is interpreted as arising from the downshift of the 1691 cm^{-1} band. The new H-bond on the C_9 keto carbonyl of P_L is somewhat stronger than that observed in the single LH(L131) mutant which was seen to vibrate at 1673 cm^{-1}.

The LH(M160) + FH(M197) double mutant was designed to introduce two new H-bonds at the C_9 keto and C_2 acetyl

carbonyls of P_M. Thus in its FT Raman spectrum (Figure 1), the 1679 cm^{-1} band, corresponding to the keto carbonyl of P_M, should downshift to *ca.* 1657 cm^{-1} and the 1653 cm^{-1} band of the acetyl carbonyl of P_M should downshift to *ca.* 1630 cm^{-1}. Figure 1 indeed shows that this spectrum lacks the 1679 cm^{-1} band and contains a new band at 1661 cm^{-1} consistent with the formation of a H-bond on the keto carbonyl of P_M. As well, this same spectrum lacks a 1653 cm^{-1} band and contains a new 1639 cm^{-1} band consistent with the formation of a new H-bond on the acetyl carbonyl of P_M. The weak band at 1676 cm^{-1}, which was masked by the intense 1679 cm^{-1} band, does not arise from P since it persists in the $P^{\bullet+}$ FT resonance Raman spectrum (see Figure 3) and is thus not attributable to neutral P. Similar observations were reported for the LH(M160) single mutant (Mattioli *et al.*, 1994). The two new H-bonds formed on P_M induce a 2 and 5 cm^{-1} perturbation of the vibrational frequencies of the C_2 and C_9 carbonyls of P_L, respectively.

Triple Mutants. The FT Raman spectrum of the primary donor in the FH(M197) + LH(L131) + LH(M160) triple mutant, for which all the acetyl and keto carbonyl groups should be H-bonded (Figure 2), essentially displays the additive features of the LH(L131) + LH(M160) double mutant and the FH(M197) single mutant. The 1636 cm^{-1} band represents the downshift of the 1653 cm^{-1} band, indicating that a H-bond has been formed on the acetyl carbonyl of P_M, as seen in the FH(M197) single mutant. The band at 1628 cm^{-1} is assigned to the C_2 acetyl carbonyl of P_L. Compared to WT, it has upshifted by 8 cm^{-1} indicating a weakening of the H-bond with His L168. This upshift, which is too small to represent a rupture of the H-bond, was interpreted as a perturbation on the C_2 acetyl carbonyl of P_L when a H-bond was formed on the C_9 keto carbonyl of P_L in the LH(L131) single and LH(L131) + LH(M160) double mutants (Mattioli *et al.*, 1994). This perturbation is also seen in the triple mutant reported here.

The C_9 keto carbonyl region (1650−1700 cm^{-1}) of the FT Raman spectrum of the FH(M197) + LH(L131) + LH(M160) triple mutant is very similar to that of the LH(L131) + LH(M160) double mutant (Mattioli *et al.*, 1994), in which two new H-bonds were formed on the keto carbonyls of P. The same conclusion is reached with this triple mutant. The 1674 cm^{-1} band is interpreted as arising from the keto carbonyl of P_L which has downshifted from 1691 cm^{-1} in the wild type strain. This represents a 17 cm^{-1} downshift similar to what was observed for both the LH(L131) single and LH(L131) + LH(M160) double mutants. The 1663 cm^{-1} band, then, arises from the downshift of the 1679 cm^{-1} band (WT) of the keto carbonyl of P_M. This downshift is smaller than those observed in the LH(M160) single and LH(L131) + LH(M160) double mutants which both exhibited a 1657 cm^{-1} band. This indicates that the H-bond formed on the keto carbonyl of P_M in this triple mutant is slightly weaker than in the corresponding single and double mutants.

The FT Raman spectrum of the HF(L168) + LH(L131) + LH(M160) triple mutant, for which both keto groups are H-bonded and both acetyl groups are free, resembles that of the LH(L131) + LH(M160) double mutant in the keto carbonyl stretching region (Figure 2). There is an observed maximum at 1657 cm^{-1} and an unresolved shoulder at *ca.* 1676 cm^{-1}. This latter feature is more resolved in the 15 K FT Raman spectrum (data not shown); however, these bands are not as resolved as in the corresponding 15 K FT Raman spectrum of the LH(L131) + LH(M160) double mutant (Mattioli *et al.*, 1994). All of the above observations are consistent with the designed H-bond changes at the C_9 keto carbonyls. The 1620 cm^{-1} band corresponding to the H-bonded acetyl carbonyl of P_L is also absent as in the HF(L168) single mutant, indicating that this H-bond with His L168 is broken, and the vibrational frequency has increased to 1657 cm^{-1}. This spectrum is very congested because it contains four overlapping Raman bands, corresponding to the two free acetyl carbonyls and the two H-bonded keto carbonyls of P. This prevents any accurate assignment of band frequencies. However, on the basis of the spectra of the single and double mutants, we may propose a total of three components under the 1657 cm^{-1} band and one component under the *ca.* 1676 cm^{-1} shoulder. However, the broadness of the *ca.* 1676 cm^{-1} component may be indicating that indeed more than one band could be under this shoulder. Spectral deconvolution of the room temperature spectrum reveals weak features and therefore possible components, at 1668 and 1678 cm^{-1} under the shoulder. The interpretation and tentative assignments of these bands are summarized in Table 1.

FT Resonance Raman Spectra of the Oxidized Primary Donor. As previously discussed, structurally informative bands arising from $P^{\bullet+}$ are resonantly enhanced in the FT Raman spectra of oxidized RCs (Mattioli *et al.*, 1991, 1993, 1994; Wachtveitl *et al.*, 1993). In wild type *Rb. sphaeroides*, these bands are observed at 1599, 1641, and 1715 cm^{-1}. These $P^{\bullet+}$ bands arise from the downshift of the 1607 cm^{-1} band (C_aC_m stretching mode) and the upshifts of the 1620 (P_L C_2 acetyl carbonyl) and 1691 (P_L C_9 keto carbonyl) cm^{-1} bands of P, respectively. The presence of the 1641 cm^{-1} band identifies the (partially) oxidized P_L species in the $P^{\bullet+}$ FT resonance Raman spectrum. The magnitude of the upshift of the C_9 keto carbonyl frequency of P_L upon the oxidation of P can be used to estimate the degree of + charge localization on this BChl molecule. For monomeric BChl *a* in nonprotic solvents, a 32 cm^{-1} upshift is observed for the C_9 keto carbonyl stretching frequency upon one-electron oxidation (Cotton *et al.*, 1980; Mäntele *et al.*, 1988; Heald & Cotton, 1990). For the case of a non-H-bonded keto carbonyl, this 32 cm^{-1} upshift represents 100% localization of a + charge on the BChl macrocycle. In the wild type strain studied in this work, we have observed a 23 ± 1 cm^{-1} upshift of the C_9 keto carbonyl of P_L and therefore estimated that (72 ± 3)% of the + charge in $P^{\bullet+}$ resides on P_L (Mattioli *et al.*, 1994). This is in good agreement with ENDOR results (68% on P_L) obtained on the same WT strain (Rautter *et al.*, 1992). The ENDOR analysis assumes that there is no significant spin density redistribution for each macrocycle and that the only change is a redistribution between P_L and P_M; this has been verified by Rautter *et al.* (1992) for the single mutants as well as for the multiple mutants studied here (J. Rautter, F. Lendzian, and W. Lubitz, personal communication). The Raman analysis assumes that 100% localization of the + charge on a BChl *a* constituent of P results in the same shift of the keto carbonyl vibrational frequency as is observed *in vitro* for nonprotic solvents. In the following, we estimate the degree of localization of the resulting + charge on P_L in the $P^{\bullet+}$ state of the mutants, on the basis of the observed upshifts of the P_L C_9 keto carbonyl frequency. At present, this analysis cannot be used with mutants containing the LH(L131) mutations as it requires

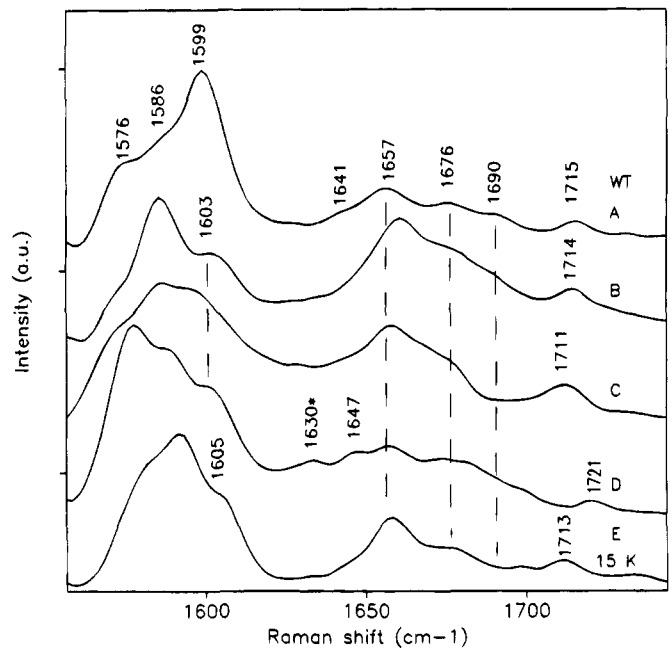

FIGURE 3: $P^{\bullet+}$ FT resonance Raman spectra of wild type and mutant RCs from *Rb. sphaeroides*: (A) wild type, (B) HF(L168) + LH(L131), (C) HF(L168) + FH(M197), and (D) LH(M160) + FH(M197). RCs were poised in their $P^{\bullet+}$ state with ferricyanide (same experimental conditions as in Figure 1). Spectrum E is of HF(L168) + LH(L131) + LH(M160) mutant at 15 K. The $P^{\bullet+}$ state was obtained by rapid freezing under constant illumination.

the C_9 keto carbonyl group of P_L not being H-bonded.

Oxidized LH(M160) + FH(M197) Double Mutant. The room temperature FT resonance Raman spectrum (Figure 3)- of the LH(M160) + FH(M197) double mutant exhibits 1647 and 1721 cm^{-1} bands. These bands indicate that the positive charge is still predominantly localized on P_L. They are both slightly higher in frequency than their counterparts in the WT spectrum at 1641 and 1715 cm^{-1}, respectively. The observed shift of the C_9 keto carbonyl of P_L upon $P^{\bullet+}$ formation is accordingly greater for this mutant (25 cm^{-1}) than for the WT (23 cm^{-1}); from this shift we estimate that 78% of the + charge resides on P_L for the LH(M160) + FH(M197) double mutant, as compared to 72% for the wild type strain. For the single mutants LH(M160) and FH-(M197), the estimated degrees of + charge localization on P_L were 80% and 75%, respectively.

Oxidized HF(L168) + FH(M197) Double Mutant. In the room temperature FT resonance Raman spectrum of this mutant (Figure 3) there is no clear band observable at *ca.* 1640 cm^{-1}, as was the case for the HF(L168) single mutant; this is entirely consistent with the assignment that this band arises from the upshift of the 1620 cm^{-1} band corresponding to the H-bonded acetyl carbonyl of P_L in the WT strain (Mattioli *et al.*, 1994). In the C_9 keto carbonyl region there is a clear band observed at 1711 cm^{-1}. Assuming that this band has upshifted by 22 cm^{-1} from 1689 cm^{-1}, corresponding to the P_L keto carbonyl in the neutral P FT Raman spectrum, the localization of the unpaired spin density on P_L would amount to 68% as was also estimated for the HF-(L168) single mutant (Mattioli *et al.*, 1994).

Oxidized HF(L168) + LH(L131) Double and HF(L168) + LH(L131) + LH(M160) Triple Mutants. The room temperature FT resonance Raman spectrum of $P^{\bullet+}$ for the HF(L168) + LH(L131) double mutant and that at 15 K for the HF(L168) + LH(L131) + LH(M160) triple mutant are shown in Figure 3. For this triple mutant, the $P^{\bullet+}$ state was achieved by trapping this state by white light illumination followed by rapid freezing. For these two mutants there is no observable band at *ca.* 1640 cm^{-1} which is characteristic of mutants bearing the FH(L168) mutation. In the C_9 keto carbonyl region, a band is observed at 1714 and 1713 cm^{-1} for the HF(L168) + LH(L131) double mutant and the HF-(L168) + LH(L131) + LH(M160) triple mutant, respectively. The additional H-bond with the C_9 keto carbonyl of P_L which has been introduced in these mutants prevents reliable estimation of the degree of + charge localization on P_L; this would require detailed experimental data on an oxidized BChl *a* molecule with the C_9 keto carbonyl engaged in a H-bond.

Optical Spectroscopy. Low-temperature (20 K) optical spectra of the reduced mutant RCs were similar to those of wild type, indicating that the structure of the protein is largely unchanged (Figure 4). Differences were observed in some of the mutants in the position and shape of the lowest, excitonic Q_y absorption band of the dimer and in the number of resolved transitions in the *ca.* 800 and 600 nm absorption bands. In low-temperature spectra, the lowest dimer Q_y band, at *ca.* 800 nm for WT, is red-shifted by *ca.* 10 nm for the LH(M160) and LH(L131) single mutants, as well as the LH-(L131) + LH(M160) and LH(M160) + FH(M197) double mutants. In contrast, for the HF(L168) and LH(L131) + HF(L168) mutants, this band was blue-shifted by *ca.* 20 nm, and in the HF(L168) + LH(M160) and HF(L168) + FH-(M197) double mutants, this band was shifted by *ca.* 40 nm to the blue. The blue shift of the dimer band in these mutants was also observed in the room temperature optical absorption spectra (Lin *et al.*, 1994). Thus, for most of the mutants the peak position of the P/P* transition changes by less than 8 nm compared to that of wild type, although some small red shifts of 5−8 nm were observed for the mutations involving H-bonding to the C_9 keto carbonyl groups. Larger shifts of 20−40 nm to the blue are noted for mutants with the loss of the H-bond between P and His L168.

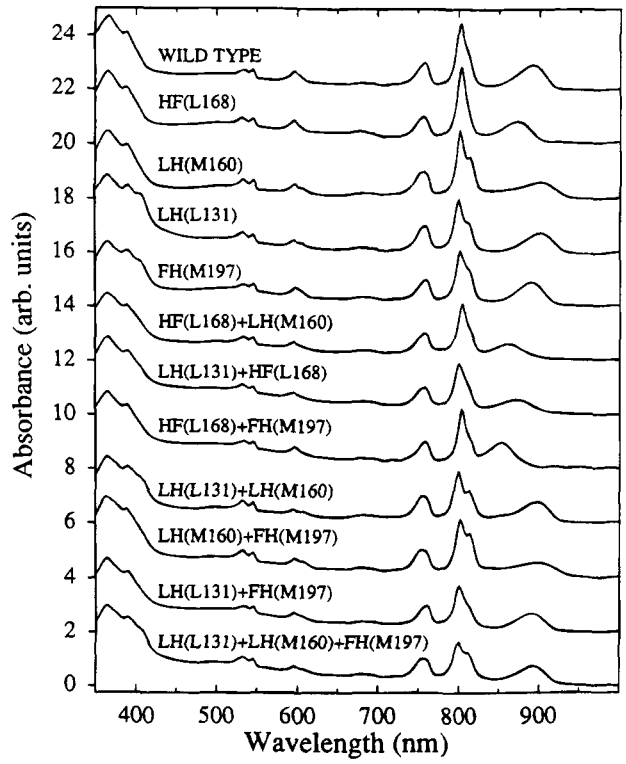

FIGURE 4: Low-temperature optical spectra of reaction centers isolated from wild type and the hydrogen bond mutants. The spectra are largely unchanged compared to that of wild type. Additional resolved transitions at *ca.* 600 and *ca.* 815 nm are evident in the spectra of some mutants compared to wild type. The P/P* transition is centered at *ca.* 890 nm in wild type and is shifted 20–40 nm to the blue or *ca.* 10 nm to the red for some of the mutants. The spectra are normalized at 760 nm.

In the wild type spectrum, a major peak is observed at 800 nm, which has a shoulder on the red side. In the LH(M160) single mutant, as well as the LH(L131) + LH(M160) and LH(M160) + FH(M197) double mutants, a well-resolved transition was observed at *ca.* 815 nm in addition to the peak at 800 nm. A more pronounced shoulder was also observed in the spectra of the LH(L131) and FH(M197) single mutants, as well as the LH(L131) + FH(M197) double mutant and the LH((L131) + LH(M160) + FH(M197) triple mutant. In contrast, in the HF(L168) single mutant, this shoulder was essentially absent. Similar additional resolved transitions were observed in the 600 nm band. These changes in the optical spectra probably reflect an alteration of the electronic structure of the bacteriochlorophyll dimer as a result of the H-bonding interactions as discussed previously (Williams *et al.*, 1992b; Murchison *et al.*, 1993).

Near-Infrared Absorption Spectra of $P^{\bullet+}$. The room temperature electronic absorption spectra of the WT and some mutant RCs in the 700–1400 nm spectral region are shown in Figure 5. Table 2 lists the maxima of this transition for all the single, double, and triple mutants. The $P^{\bullet+}$ transition at *ca.* 1250 nm is seen to significantly red-shift when a histidine-donated H-bond is present on a C_9 carbonyl group of P, *i.e.*, in the mutant strains with LH(M160) and LH(L131) mutations. In contrast, introducing such H-bonds on the C_2 acetyl carbonyls of P leaves the position of this band essentially unaltered (*i.e.*, mutants containing the HF(L168) and FH(M197) single mutations). Furthermore, with reference to the single mutants, the shifts exhibited in the double and triple mutants are essentially additive, save for one exception, the LH(M160) + FH(M197) double mutant, where the observed red shift is 19 nm with respect to WT and a shift of 10 nm is predicted for the case of additivity.

DISCUSSION

The breaking and formation of H-bonds involving histidine residues with the conjugated carbonyl groups of the primary donor of *Rb. sphaeroides* results in specific changes in its redox potential (Lin *et. al.*, 1994a). The range of midpoint potentials observed for the mutants reported here vary from 410 mV (no H-bonds on P) to 765 mV (all four conjugated carbonyls H-bonded). This large range of 355 mV results from the additive effects of the single mutations. Despite this large change in redox potential of P, RCs isolated from all strains are still capable of electron transfer to the quinones.

The large changes in P redox midpoint potentials do not correlate with any of the changes in the dimer band corresponding to the P/P* electronic transition (Figure 4). This point is illustrated by the similarity of the P/P* absorption maxima, at 893 nm, of WT and the HF(L168) + LH(L131) + LH(M160) triple mutant (Figure 4) and Table 2); the absorption maxima are virtually identical, yet the $P/P^{\bullet+}$ redox potentials differ by 260 mV. These observations indicate that these H-bonds may have little effect on the energy of the first excited electronic state of P relative to the ground state. This would imply that the stabilization of the P ground state due to the H-bonds is very near to that of the P* state. In this interpretation, the increase in $P/P^{\bullet+}$ redox potential could arise from the decreased stability, due to H-bonding, of the $P^{\bullet+}$ relative to the ground state (Lin *et al.*, 1994a).

The HF(L168) + LH(M160) and HF(L168) + FH(M197) mutants show significant blue shifts of the lowest Q_y dimer band of 30 and 40 nm, respectively. On the basis of INDO calculations, Hanson and co-workers (Hanson *et al.*, 1987) have predicted spectral changes on the order of *ca.* 10 nm in the Q_y absorption band of BChl species forming H-bonds on the C_2- or C_9-conjugated carbonyls; greater shifts could be expected if the carbonyl groups are polarized by H-bonding [see Scherz *et al.* (1991)]. Also, both extended Hückel and INDO calculations (Hanson *et al.*, 1987) have indicated that H-bonding at the C_9 keto carbonyl group of a BPhe *a* molecule could alter its reduction potential by 40 mV; however, parameters such as the strength of the H-bond used in the calculation were not specified. From Figure 4, it is clear that mutations incorporating the HF(L168) alteration show the largest effect on the P/P* dimer band and always to higher energies; the HF(L168) + FH(M197) double mutant exhibits the largest blue shift of all the mutants studied here. The FH(M197) single mutation does not significantly alter the RC optical absorption spectrum but results in the largest single change in $P/P^{\bullet+}$ redox midpoint potential (125 mV relative to wild type) even though the H-bond this mutation introduces is not as strong as that found with His L168 in native RCs.

Histidine L168, which forms a H-bond with the C_2 acetyl carbonyl of P_L, is conserved in several species of purple bacteria including *Rhodopseudomonas viridis*, *Rhodospirillum rubrum*, and *Rhodobacter capsulatus* (Komiya *et al.*, 1988). This H-bond, as observed in the FT Raman spectra of P in *Rb. sphaeroides* (strains R26 and 2.4.1 and from this work), *Rb. capsulatus*, and *Rsp. rubrum* (Mattioli *et al.*, 1992)

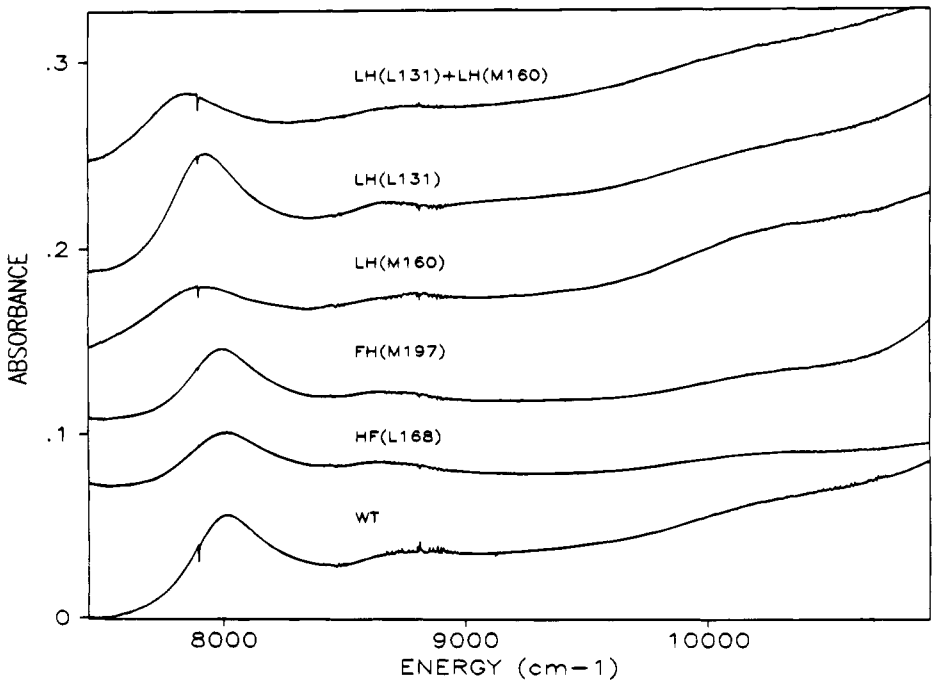

FIGURE 5: Room temperature absorption spectra of oxidized wild type and some of the hydrogen bond mutants, in the near-infrared spectral region. These spectra were normalized at 800 nm. The major band in this region is centered at *ca.* 8000 cm^{-1} (1250 nm) for wild type. The peak positions (in nm) for these and the other mutants are listed in Table 2.

Table 2. Observed Maxima of P and $P^{\bullet+}$ Electronic Transition (nm)

strain	P* [a]	Δ[a]	P•+* [b]	Δ[b]
WT	893		1250	
HF(L168)	873	−20	1248	−2
FH(M197)	890	−3	1250	0
LH(M160)	900	7	1260	10
LH(L131)	901	8	1264	14
LH(L131) + LH(M160)	898	5	1277	27
HF(L168) + LH(L131)	873	−20	1261	11
HF(L168) + FH(M197)	853	−40	1247	−3
LH(M160) + FH(M197)	899	6	1269	19
HF(L168) + LH(M160)[c]	863	−30	nd	
LH(L131) + FH(M197)[c]	890	−3	nd	
FH(M197) + LH(L131) + LH(M160)	893	0	1276	26
HF(L168) + LH(L131) + LH(M160)	870	−23	1277	27

[a] Low-temperature (15 K) data. [b] Room temperature data. [c] Room temperature Raman and near-IR absorption data not obtained for these mutants.

shifts the acetyl carbonyl stretching frequency down to 1620 cm^{-1}, which reflects one of the strongest H-bonds observed to date to involve a conjugated carbonyl of a BChl *a* molecule in a protein. It seems likely then that this highly conserved His L168 could be responsible, in addition to specifically tuning the redox properties of P, for maintaining a specific geometry of P_L with respect to P_M. Once the His L168 H-bond to the acetyl carbonyl is removed, P_L and P_M could modestly reposition themselves with respect to one another and therefore blue-shift the dimer band. Although no significant blue shift of the dimer band is observed in the absorption spectrum of the FH(M197) single mutant when a new H-bond is introduced to the acetyl group of P_M via histidine at position M197, the combination of this additional H-bond with the removal of the H-bond to the acetyl carbonyl group of P_L in the HF(L168) + FH(M197) double mutant could sufficiently reposition P_L with respect to P_M so as to result in a 40 nm blue shift of the dimer band of this double mutant. Contributions to the observed blue shift could also arise from possible changes in the geometry of the acetyl carbonyl groups with respect to the macrocycle [as modeled by Plato *et al.* (1986); Parson & Warshel, 1987).

In contrast to the effects of the mutations on the wavelength of the *ca.* 890 nm dimer Q_y absorption band corresponding to the P/P* transition, the *ca.* 1250 nm absorption band corresponding to $P^{\bullet+}$ is shifted due to mutations near the C_9 keto carbonyl groups and not near the C_2 acetyl groups. This shift of the 1250 nm band is independent of which side of the dimer is preferentially stabilized. These observations imply that a critical factor for the shift of the 1250 nm band is either the orientation of the imidazole ring of histidine relative to the dimer or the position of the H-bond relative to the Q_y transition moment. The nature of this 1250 nm electronic transition is not fully understood. On the basis of Stark effect spectroscopy of this band, Stocker *et al.* (1993) concluded that the corresponding electronic transition is delocalized over P_L and P_M. Recently, two models have been presented to describe this transition. Parson *et al.* (1992) have described it as an intramolecular transition using a simple quantum mechanical model with dimer molecular orbital basis states in which the + charge of $P^{\bullet+}$ is localized on either P_L or P_M. Reimers and Hush (1995) have suggested the alternative assignment of a transition between the ground state and an excited triplet state that is coupled to electron exchange. Both models predict that the energy of the transition should be insensitive to changes in the energy of P_L^+ relative to P_M^+ which is consistent with our observations of only small shifts in the position of this transition in the mutants. In addition, the models predict that the strength of the transition should be very sensitive to structural distortions. Since the observed oscillater strengths are all very similar, the models are consistent with the mutations causing only minor structural changes. An understanding of the reason for the small

observed shifts would require more detailed models than presently available.

The FT Raman spectral assignments for mutants with multiple changes can be consistently made that are in excellent agreement with the designed changes and observed single-site spectral changes (Mattioli *et al.*, 1994). Furthermore, the FT Raman data presented here established two important points concerning these mutants. Firstly, all H-bonds designed to be formed or removed by site-directed mutagenesis have been verified from the vibrational spectra of the primary donors in these mutant RCs. Secondly, these changes in H-bond interactions in the double and triple mutants appear to be of similar strengths as compared to the single mutants. In other words, not only are the H-bonds formed and broken in the double and triple mutants but their bond strengths are, in general, conserved in the multiple mutations. These results correlate with the specific changes in the redox potential of the $P/P^{\bullet+}$ couple and the additive manner in which the multiple combinations of the single mutations alter the P redox potential (Lin *et al.*, 1994a,b).

Correlation between Total H-Bond Interaction and $P/P^{\bullet+}$ Redox Potential. The frequencies of the carbonyl stretching modes are sensitive to the strengths of H-bonding which can be quantitated by the H-bond enthalpy, ΔH; the greater the observed downshift in carbonyl vibrational frequency, the more negative the ΔH value. The magnitude of ΔH directly reflects the interaction energy between the H-bond donor and acceptor; this interaction energy represents the difference in energy between the H-bonded donor−acceptor complex and the isolated, noninteracting pair of donor and acceptor molecules (Latajka & Scheiner, 1990). In general, the enthalpy of formation of a H-bond is linearly related to the shift in vibrational frequency of the chemical groups engaged in such a bond (Badger & Bauer, 1937). Such thermodynamic correlations have been often observed [Joesten & Schaad, 1974; Tonge & Carey, 1992; see review in Callender and Deng (1994)]. The exact form of the linear relationship depends on the specific system studied.

To quantitate the strengths of the H-bonds formed or broken with P in the mutant RCs, one needs to determine ΔH values that correspond to the observed vibrational frequency shifts of the C_2 and C_9 carbonyl groups. One approach is to use experimentally determined ΔHs corresponding to carbonyl frequency shifts observed in model systems consisting of model compounds in solution equilibrium with H-bond donors. In a series of such model systems where for each system donor and acceptor are changed in order to obtain a broad range of ΔH and frequency shift values, an empirically determined ΔH versus carbonyl frequency shift relationship can be obtained and then used to gauge or calibrate the observed vibrational frequency shifts in the protein with a ΔH value. Such a relationship between H-bond enthalpy, ΔH, and carbonyl vibrational frequency shifts was experimentally obtained by Zadorozhnyi and Ishchenko (1965) for aromatic carbonyl compounds; these compounds begin to approximate the π-conjugated carbonyl groups of chlorophylls but are strictly not accurate, yet these model compounds should represent a good estimate of the true H-bond enthalpies of chlorophylls. Nonetheless, a linear relationship between H-bond enthalpy and shifts of chlorophyll carbonyl group frequencies is expected.

For a particular frequency shift in C_2 or C_9 carbonyl group of P observed for the mutant RCs, we have used the corresponding ΔH value from the ΔH versus carbonyl frequency shift relationship of Zadorozhnyi and Ishchenko (1965) to estimate the true value which would be needed to correctly reflect the observed vibrational frequency shift of the P carbonyl group. This was done for each and every carbonyl frequency shift in the mutant spectra. For the mutants, the ΔH values associated with the rupture of existing H-bonds or the formation of new H-bonds result in changes in H-bonding interactions represented by a change in ΔH with respect to wild type, $\Delta\Delta H$. The calculated value $\Delta\Delta H$ represents the difference in H-bonding interaction energy between P and the protein for the cases of 0−4 H-bonds, all with respect to wild type. These values are listed in Table 1. The WT case is taken as a zero-point reference, *i.e.*, no change in H-bond interaction or enthalpy ($\Delta\Delta H = 0$). For the case of the HF(L168) mutant, since a H-bond is broken, the estimated change in H-bond enthalpy, $\Delta\Delta H$, is taken as "negative" with respect to WT. For the double and triple mutants, the estimated ΔHs of each single H-bond (based on the observed shift of each single carbonyl group) are added to give an estimated total change in H-bond enthalpy with respect to WT. When the above values are compared to the observed change in $P/P^{\bullet+}$ redox midpoint potential, a definite correlation is observed. This correlation is best illustrated in Figure 6 which shows the change in the $P/P^{\bullet+}$ redox midpoint potential relative to WT plotted as a function of the total change in H-bond interaction energy (enthalpy). This plot can be fit to a straight line with a slope of 0.59 mV/meV and an intercept of 32 mV, with a correlation coefficient of 0.954. Because of the ambiguity of the band assignments for the congested FT Raman spectrum of the HF(L168) + LH(L131) + LH(M160) triple mutant, as previously discussed (see Results), two possible changes in calculated total change in enthalpy, −44 meV in one case and 25 meV for the other, were proposed for this mutant (Table 1). Inclusion of these two data points for the HF(L168) + LH(L131) + LH(M160) triple mutant does not significantly alter the curve in Figure 6.

The line in Figure 6 spans a total redox midpoint potential range of 360 mV and a H-bond enthalpy range of *ca.* 450 meV. It indicates a linear correlation between the redox potential of P and the cumulative enthalpies of H-bonds on the C_2 and C_9 carbonyl groups, however with some significant scatter. This correlation *implies* that the strength of the H-bonds on P largely determines the change in its redox potential. For example, two H-bonds would have an identical effect as a single H-bond that was twice as strong. Moreover, the change in this interaction energy is close to the change in oxidation potential; thus changes in interaction energy scale nearly identically with the change in redox potential. Since there are four conjugated carbonyl groups contributing to the total interaction energy, for the purposes of such a curve, the primary donor can be considered as a strongly coupled system or a single supermolecule where increasing this interaction energy with the protein via multiple H-bonds to P alters its redox potential.

This curve strictly applies to H-bonds formed on P of *Rb. sphaeroides* donated by histidine residues and may not represent a general tendency for all amino acid residues. For example, a H-bond donated by a tyrosine introduced via the mutation FY(M197) in *Rb. sphaeroides* RCs resulted in only

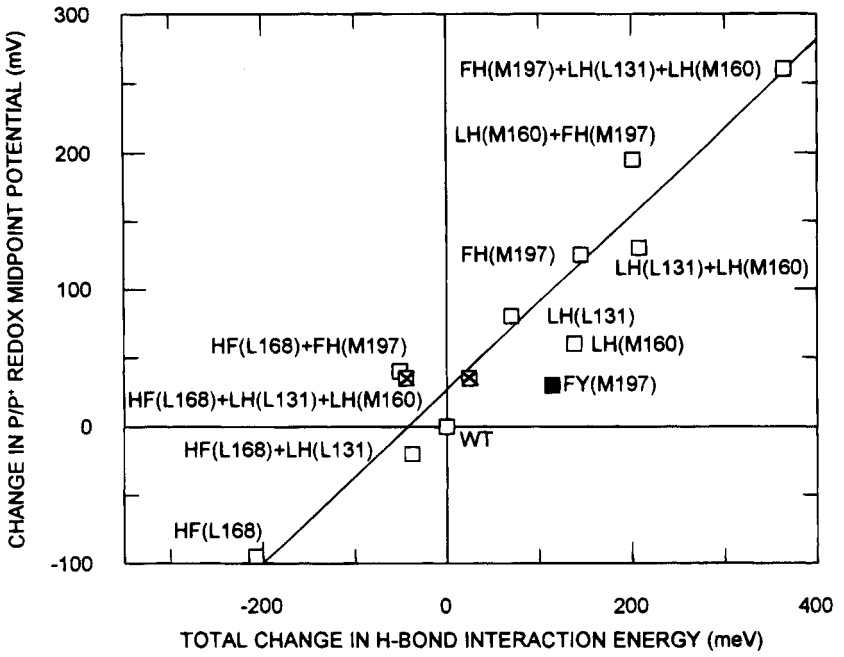

FIGURE 6: Change in $P/P^{\bullet+}$ redox midpoint potential of the hydrogen bond mutants relative to wild type, plotted as a function of the total change in hydrogen-bonding interaction as gauged by the estimated hydrogen bond enthalpies deduced from observed shifts of the stretching frequency of the conjugated carbonyl of P. Data points are taken from Table 1. The line shown represents a linear regression fit with $r = 0.954$ and does not include the two data points from the HF(L168) + LH(L131) + LH(M160) mutant (□ with ×) and that from the FY(M197) mutant (■) (Wachtveitl *et al.*, 1993). Inclusion of these three data points does not significantly change the line.

a modest *ca.* 30 mV change in the $P/P^{\bullet+}$ redox midpoint potential (Wachtveitl *et al.*, 1993), whereas the FH(M197) mutant discussed here displays the largest changes (125 mV compared to wild type) in midpoint potential due to a single mutation. This observation was interpreted as possibly arising from the difference in the chemical nature of the H-bond donor. The scattering seen in Figure 6 could arise from additional local electrostatic interactions other than the H-bond.

In general, the change in $P/P^{\bullet+}$ redox midpoint potential seems closely related to the H-bonding interaction energy which is expected to stabilize the ground state of P. The work presented here identifies and initially characterizes H-bonding as a type of protein interaction which contributes to the tuning of redox potentials of chlorophylls. To date, most discussions concerning the role of the protein in tuning the redox properties of cofactors generally address systems where the change in oxidation state involves a metal (*e.g.*, cytochromes, blue copper proteins, iron–sulfur clusters), where certainly the effects of metal coordination are a major influence on the cofactor redox potential [see review in Wuttke and Gray (1993); Jensen *et al.*, 1994). The H-bonding interactions described in this work raise the redox potential of chlorophylls for which oxidation involves extraction of an electron that is not localized on the Mg^{2+} metal but rather is distributed over the macrocycle.

ACKNOWLEDGMENT

We thank Kelly Carty for protein purification.

REFERENCES

Allen, J. P., Feher, G., Yeates, T. O., Komiya, H., & Rees, D. C. (1987) *Proc. Natl. Acad. Sci. U.S.A. 84*, 5730–5734.

Badger, R. M., & Bauer, S. H. (1937) *J. Chem. Phys. 5*, 839–855.

Beekman, L. M. P., Visschers, R., Monhouser, R., van Mourik, F., Heer-Dawson, M., Mattioli, T. A., McGlynn, P., Hunter, C. N., Robert, B., van Grodelle, R., & Jones, M. R. (1995) (submitted for publication).

Callender, R., & Deng, H. (1994) *Annu. Rev. Biophys. Biomol. Struct. 23*, 215–245.

Chirino, A. J., Lous, E. J., Huber, M., Allen, J. P., Schenck, C. C., Paddock, M. L., Feher, G., & Rees, D. C. (1994) *Biochemistry 33*, 4584–4593.

Cotton, T. M., Parks, K. D., & Van Duyne, R. P. (1980) *J. Am. Chem. Soc. 102*, 6399–6407.

El-Kabbani, O., Chang, C.-H., Tiede, D., Norris, J., & Schiffer, M. (1991) *Biochemistry 30*, 5361–5369.

Ermler, U., Fritzsch, G., Buchanan, S. K., & Michel, H. (1994) *Structure 2*, 925–936.

Feiler, U., & Hauska, G. (1994) in *Anoxygenic Photosynthetic Bacteria* (Blankenship, R. E., Madigan, M. T., & Bauer, C. E., Eds.) Kluwer, Dordrecht (in press).

Hanson, L. K., Thompson, M. A., & Fajer, J. (1987) in *Progress in Photosynthesis Research* (Biggins, J., Ed.) Vol. I, pp 311–314, Martinus Nijhoff, Dordrecht, The Netherlands.

Heald, R. L., & Cotton, T. M. (1990) *J. Phys. Chem. 94*, 3968–3975.

Jensen, G. M., Warshel, A., & Stephens, P. J. (1994) *Biochemistry 33*, 10911–10924.

Jia, Y., DiMagno, T. J., Chan, C.-K., Wang, Z., Du, M., Hanson, D. K., Schiffer, M., Norris, J. R., & Fleming, G. R. (1993) *J. Phys. Chem. 97*, 13180–13191.

Joesten, M., & Schaad, L. J. (1974) *Hydrogen Bonding*, Marcel Dekker, New York.

Komiya, H., Yeates, T. O., Rees, D. C., Allen, J. P., & Feher, G. (1988) *Proc. Natl. Acad. Sci. U.S.A. 85*, 9012–9016.

Latjka, Z., & Scheiner, S. (1990) *Chem. Phys. Lett. 174*, 179–184.

Lin, X., Murchison, H. A., Nagarajan, V., Parson, W. W., Williams, J. C., & Allen, J. P. (1994a) *Proc. Natl. Acad. Sci. U.S.A. 91*, 10265–10269.

Lin, X., Williams, J. C., Allen, J. P., & Mathis, P. (1994b) *Biochemistry 33*, 13517–13523.

Mäntele, W. G., Wollenweber, A. M., Nabedryk, E., & Breton, J. (1988) *Proc. Natl. Acad. Sci. U.S.A. 85*, 8468–8472.

Mattioli, T. A., Hoffmann, A., Robert, B., Schrader, B., & Lutz, M. (1991) *Biochemistry 30*, 4648–4654.

Mattioli, T. A., Robert, B., & Lutz, M. (1992) in *The Photosynthetic Bacterial Reaction Center: Structure, Spectroscopy, and Dynam-*

ics (Breton, J., & Vermeglio, A., Eds.) pp 127−132, Plenum, New York.
Mattioli, T. A., Hoffmann, A., Sockalingum, D., Schrader, B., Robert, B., & Lutz, M. (1993) *Spectrochim. Acta 49A*, 785−799.
Mattioli, T. A., Williams, J. C., Allen, J. P., & Robert, B. (1994) *Biochemistry 33*, 1636−1643.
Moss, D. A., Leonhard, M., Bauscher, M., & Mäntele, W. (1991) *FEBS Lett. 283*, 33−36.
Murchison, H. A., Alden, R. G., Allen, J. P., Peloquin, J. M., Taguchi, A. K. W., Woodbury, N. W., & Williams, J. C. (1993) *Biochemistry 32*, 3498−3505.
Nabedryk, E., Allen, J., Taguchi, A., Williams, J., Woodbury, N., & Breton, J. (1993) *Biochemistry 32*, 13879−13885.
Nagarajan, V., Parson, W. W., Davis, D., & Schenck, C. C. (1993) *Biochemistry 32*, 12324−12336.
Nitschke, W., & Rutherford, A. W. (1991) *Trends Biochem. Sci. 16*, 241−245.
Parson, W. W., & Warshel, A. (1987) *J. Am. Chem. Soc. 109*, 6152−6163.
Parson, W. W., Nabedryk, E., & Breton, J. (1992) in *The Photosynthetic Bacterial Reaction Center: Structure, Spectroscopy, and Dynamics* (Breton, J., & Vermeglio, A., Eds.) pp 79−88, Plenum, New York.
Plato, M., Trankle, E., Lubitz, W., Lendzian, F., & Möbius, K. (1986) *Chem. Phys. 107*, 185−196.
Rautter, J., Gessner, Ch., Lendzian, F., Lubitz, W., Williams, J. C., Murchison, H. A., Wang, S., Woodbury, N. W., & Allen, J. P. (1992) in *The Photosynthetic Bacterial Reaction Center: Structure, Spectroscopy, and Dynamics* (Breton, J., & Vermeglio, A., Eds.) pp 99−108, Plenum, New York.
Reimers, J. R., & Hush, N. S. (1995) *J. Am. Chem. Soc. 117*, 1302−1308.
Scherz, A., Rosenbach-Belkin, V., & Fisher, J. R. E. (1991) in *The Chlorophylls* (Scheer, H., Ed.) pp 237−268, CRC Press, Boca Raton, FL.
Stocker, J. W., Hug, S., & Boxer, S. G. (1993) *Biochim. Biophys. Acta 1144*, 325−330.
Tonge, P. J., & Carey, P. R. (1992) *Biochemistry 31*, 9122−9125.
Wachtveitl, J., Farchaus, J. W., Das, R., Lutz, M., Robert, B., & Mattioli, T. A. (1993) *Biochemistry 32*, 12875−12886.
Watanabe, T., & Kobayashi, M. (1991) in *The Chlorophylls* (Scheer, H., Ed.) pp 287−315, CRC Press, Boca Raton, FL.
Williams, J. C., Alden, R. G., Coryell, V. H., Lin, X., Murchison, H. A., Peloquin, J. M., Woodbury, N. W., & Allen, J. P. (1992a) in *Research in Photosynthesis* (Murata, N., Ed.) Vol. I, pp 377−380, Kluwer, Dordrecht.
Williams, J. C., Alden, R. G., Murchison, H. A., Peloquin, J. M., Woodbury, N. W., & Allen, J. P. (1992b) *Biochemistry 31*, 11029−11037.
Woodbury, N. W., Lin, S., Lin, X., Peloquin, J., Taguchi, A. K. W., Williams, J. C., & Allen, J. P. (1995) *Chem. Phys.* (submitted for publication).
Wuttke, D. S., & Gray, H. B. (1993) *Curr. Opin. Struct. Biol. 3*, 555−563.
Yeates, T. O., Komiya, H., Chirino, A., Rees, D. C., Allen, J. P., & Feher, G. (1988) *Proc. Natl. Acad. Sci. U.S.A. 85*, 7993−7997.
Zadorozhnyi, B. A., & Ishchenko, I. K. (1965) *Opt. Spectrosc. (Engl. Transl.) 19*, 306−308.

BI942930Z